PRAMANA
— journal of
physics

Vol. 70, No. 1
January 2008
pp. 101–111

Proton radioactivity with analytically solvable potential

I MEHROTRA and S PRAKASH*
Department of Physics, University of Allahabad, Allahabad 211 002, India
*Corresponding author
E-mail: indum81@gmail.com; shwetap75@rediffmail.com

MS received 19 December 2006; revised 2 August 2007; accepted 14 August 2007

Abstract. The phenomenon of proton emission is treated as a process of asymmetric fission through a one-dimensional potential barrier developed due to combined effects of the Coulomb potential, centrifugal potential and various renormalization processes. The barrier is simulated to an asymmetric, smooth and analytically solvable potential with adjustable depth, shape and range. The half-lives of proton emitters in the mass range $A = 105$–171 have been calculated using exact expression for the transmission coefficients. Good agreement with the experimental data is obtained by the adjustment of just one parameter in all the cases.

Keywords. Proton radioactivity; half-life; tunneling.

PACS Nos 23.50.+z; 23.90.+w; 27.60.+j; 27.70.+q

1. Introduction

The recent developments of radioactive nuclear beams have opened up the possibility of exploring a wide variety of nuclei far from the valley of β-stability. The proton drip line defines one of the fundamental limits to nuclear stability. Nuclei lying on or beyond this line are energetically unbound to the emission of a constituent proton. Ground state proton emitters have been discovered in the masses around 100, 150 and 190 [1]. In the light of this, various theoretical studies have been carried out to study the proton radioactivity from proton-rich nuclei [2]. The existing theoretical studies can be classified into two broad categories. In the first category different theoretical approaches are based on quantum mechanical foundation such as transmission through a potential barrier [3], distorted wave Born approximation [4] and the perturbative methods [5]. In all these methods it is assumed that the proton moves in an effective spherical potential with a barrier, which in turn is obtained by considering the interaction of the proton with the remaining core nucleons. It comprises of a nuclear optical potential, the Coulomb potential and the centrifugal potential. The proton optical potential is approximated by an

average Woods–Saxon field containing the central and the spin-orbit potential terms. Half-lives of nuclei with A ranging from 105 to 171 have been calculated and good agreement with existing data is obtained [2,3].

In the second category attempts have been made to unify the processes of α-decay, cluster radioactivity, cold fission and proton radioactivity by using models which project the multidimensional fragmentation part into the one-dimensional motion to allow the calculations of Gamow penetrability factor [6,7]. It has been conventional to treat the particle decay and α-decay of nuclei using quantum mechanical methods, while fission was studied on the basis of liquid drop model. After Strutinsky's hybrid model [8] attempts were made to understand fission on the basis of microscopic methods. Thus α-decay or any other particle decay can be considered as a process of a very asymmetric fission and fission barrier is obtained by modifications in the gross liquid drop model potential arising due to various physical processes. In the work of Guzmann *et al* [9] the barrier potential is formed by Coulomb potential and effective surface potential in which nuclear structure effects are included by means of experimental Q values and configuration-dependent inertia coefficients. The multidimensional evolution of the system is reduced to one-dimensional case by geometrical and incompressibility constraints. The resulting effective potential barrier exhibits a small inner tail. These authors have calculated the half-lives of nuclei with A ranging from 105 to 165 and have obtained values which are in good agreement with the existing data. Shanmugam *et al* [10] have developed a cubic inner barrier joined smoothly to an outer barrier of Yukawa plus exponential form. They have used this to calculate the half-lives of proton emitters with mass A ranging from 105 to 171. Thus in general there are different approaches for calculating the potential barrier but in all the cases the barrier can be separated into an internal part (when the separation between nascent fragments is smaller than the touching distance) and the external part (when the fragment separation is greater than the touching distance).

In the present work, following second line of approach, proton decay is considered as a process of asymmetric fission through a barrier. This barrier is represented by a highly versatile form of the potential developed by Sahu *et al* [11,12]. The potential is smooth, analytically solvable and has three parameters which control the height, range and flatness at the top. The asymmetric nature of the barrier is constructed by placing side by side two such potentials of different parameters, one representing the internal part and the other the external part and matching their heights at the touching distance. By varying the set of six parameters a variety of potentials can be generated and the versatile nature can account for various processes which renormalize the potential. The above potential has been used to calculate the half-lives of proton emitters with $A = 105$–171 using the exact expression for the transmission coefficient across the barrier. In §2 we describe the main features of our model. In §3 model parameters are given. The results obtained are given in §4. Section 5 gives the summary and conclusions.

2. The model

The analysis of the large number of theoretical studies indicate that the effective barrier experienced by proton gets modified from its simple Coulomb and

centrifugal form due to various physical processes like coupling between relative motion and the internal degrees of freedom, static deformation, collective vibration, inelastic excitation etc. Shi and Swiatecki [13] have shown that inclusion of the nuclear proximity attraction reduces the height of the Coulomb barrier substantially. Jenson and Wong [14] have observed that the nuclear interaction modifies the Coulomb barrier such that it has a parabolic shape near its top. Guzmann *et al* [9] have developed effective liquid drop model potential barrier for proton emission of heavy nuclei which has a small inner tail arising due to renormalization effects in the inner region. Shanmugam *et al* [10,15,16] have shown that the barrier potential in the post-scission region gets modified due to change in the nuclear interaction energy by finite range effects, quadrupole deformation of the daughter nucleus etc. Their barrier potential is represented by Yukawa plus exponential potential in the outer region, and a narrow cubic potential form given by Nix [17] in the inner region. Thus in the simplest picture where one visualizes the proton emission as basically a one-dimensional barrier transmission problem, this notion of modification of the barrier due to various renormalization processes can be incorporated by developing a versatile potential barrier with variable asymmetry, height, range and flatness at the top. In the present work we have used the versatile potential barrier developed by Sahu *et al* from Ginnochio potential [18] to describe the phenomenon of proton radioactivity. The phenomenon of proton emission reduced to one-dimensional motion of proton in an effective potential field is described by the Schrödinger equation as

$$\frac{-\hbar^2}{2\mu}\frac{\mathrm{d}^2\psi(r)}{\mathrm{d}r^2} + V(r)\psi(r) = E\psi(r), \tag{1}$$

where μ is the reduced mass of the proton-daughter nucleus system. The potential $V(r)$ has two components, inner barrier in the overlapping region ($r < C_\mathrm{t}$) and outer barrier in the non-overlapping region ($r > C_\mathrm{t}$), and are given by [12]

$$\begin{aligned} V(r) &= V_{01}[\lambda_1^2\nu_1(\nu_1+1)(1-y_1^2)+\xi_1] \quad \text{if } 0 \le r < C_\mathrm{t} \\ V(r) &= V_{02}[\lambda_2^2\nu_2(\nu_2+1)(1-y_2^2)+\xi_2] \quad \text{if } r > C_\mathrm{t} \end{aligned} \tag{2}$$

and

$$\xi_1 = \frac{1-\lambda_1^2}{4}[5(1-\lambda_1^2)y_1^4 - (7-\lambda_1^2)y_1^2 + 2](1-y_1^2),$$
$$\xi_2 = \frac{1-\lambda_2^2}{4}[5(1-\lambda_2^2)y_2^4 - (7-\lambda_2^2)y_2^2 + 2](1-y_2^2),$$

where V_{01} and V_{02} are the strengths of the potential in MeV. The parameter ν measures the height of the barrier and the parameter λ describes the shape of the barrier. C_t is the touching configuration of the two nuclei with C_i as the Susmann central radii

$$C_i = R_i - \frac{r_0^2}{R_i} \tag{3}$$

with surface radius $r_0 = 0.99$ fm, $R_i = 1.13A_i^{1/3}$ and $C_\mathrm{t} = C_1 + C_2$, $i = 1, 2$. We define a new dimensionless variable $\rho_n = (r - C_\mathrm{t})b_n$ with $b_n = \sqrt{2\mu V_0/\hbar^2}$, $n = 1, 2$. b_n has the dimensions of [length]$^{-1}$. ρ_n is related to the variable y_n as

$$\rho_n = \frac{1}{\lambda_n^2}[\tanh^{-1} y_n - (1-\lambda_n^2)^{1/2} \tanh^{-1}(1-\lambda_n^2)^{1/2} y_n]. \tag{4}$$

The ranges of variation of r, ρ_n and y_n are as follows. In the interior side r varies from 0 to C_t, ρ_1 varies from $-C_\mathrm{t}b_1$ (large) to 0 while y_1 starts with a value close to -1 and ends up with zero at $r = C_\mathrm{t}$. In the outer side, while r goes from C_t to ∞, ρ_2 varies from 0 to ∞ and hence, y_2 varies from 0 to 1. The parameters λ_1, ν_1 specify the potential in the interior region $r < C_\mathrm{t}$ and the parameters λ_2, ν_2 specify the potential in the outer region $r > C_\mathrm{t}$.

The expression of the potential on the interior side gives us the value at $r = C_\mathrm{t}(y_1 = 0)$ as the height of the barrier

$$V_{\mathrm{B}1} = V_{01}\left[\lambda_1^2\left(\nu_1^2 + \nu_1 - \frac{1}{2}\right) + \frac{1}{2}\right]. \tag{5}$$

The height of the potential at $r = C_\mathrm{t}(y_2 = 0)$ obtained for the outer region from the eq. (2) is

$$V_{\mathrm{B}2} = V_{02}\left[\lambda_2^2\left(\nu_2^2 + \nu_2 - \frac{1}{2}\right) + \frac{1}{2}\right]. \tag{6}$$

A single barrier of certain height V_B in MeV at $r = C_\mathrm{t}$ is set by taking

$$V_{01} = \frac{V_\mathrm{B}}{[\lambda_1^2(\nu_1^2 + \nu_1 - \frac{1}{2}) + \frac{1}{2}]} \tag{7}$$

and

$$V_{02} = \frac{V_\mathrm{B}}{\left[\lambda_2^2\left(\nu_2^2 + \nu_2 - \frac{1}{2}\right) + \frac{1}{2}\right]} \tag{8}$$

so that $V_{\mathrm{B}1} = V_{\mathrm{B}2} = V_\mathrm{B}$.

By varying the parameters V_B, ν and λ, the height, range and flatness at the top can be changed and a variety of potentials can be generated. Thus the highly versatile nature of the potential makes it suitable for use in the proton radioactivity study. The asymmetric potential barrier $V(r)$ is analytically solvable and exact expression for the transmission coefficient across the barrier is given as [11]

$$T = \frac{16\pi^4\lambda_1\lambda_2 h_1 h_2}{[(\lambda_2^2|L_1|^2 + \lambda_1^2|L_2|^2)(s_1^2 + h_1^2)(s_2^2 + h_2^2) + 8\pi^4\lambda_1\lambda_2(s_1 s_2 + h_1 h_2)]}, \tag{9}$$

$$s_1 = \sin(\pi\bar{\nu}_1), \quad s_2 = \sin(\pi\bar{\nu}_2), \quad h_1 = \sinh\left(\frac{\pi k_1}{\lambda_1^2}\right),$$
$$h_2 = \sinh\left(\frac{\pi k_2}{\lambda_2^2}\right), \quad k_1 = \sqrt{\frac{Q}{V_{01}}}, \quad k_2 = \sqrt{\frac{Q}{V_{02}}},$$

where

$$\bar{\nu}_1 = \left[\frac{1}{4} - \nu_1(\nu_1+1) + \frac{\lambda_1^2-1}{\lambda_1^4}k_1^2\right]^{1/2} - \frac{1}{2},$$
$$\bar{\nu}_2 = \left[\frac{1}{4} - \nu_2(\nu_2+1) + \frac{\lambda_2^2-1}{\lambda_2^4}k_2^2\right]^{1/2} - \frac{1}{2}. \tag{10}$$

The above expression is applicable for $\ell = 0$ angular momentum state of the emitted proton. For higher angular momentum states an additional centrifugal term $V_\ell = [\hbar^2/2\mu]\ell(\ell+1)/r^2$ should be incorporated in the Schrödinger eq. (1). As it is not possible to solve exactly the Schrödinger equation with this potential V_ℓ incorporated in the potential given by eq. (1), we approximately incorporate the effect of this term by making the ℓ-dependence as follows:

(i) s-wave height $V_{\rm B}$ at $\rho = 0$ is replaced by the partial wave height

$$V_{{\rm B}\ell} = V_{\rm B} + \frac{\hbar^2}{2\mu}\frac{\ell(\ell+1)}{C_{\rm t}^2}. \tag{11}$$

(ii) The parameters $\nu_{1\ell}$ and $\nu_{2\ell}$ describing the range of the potential in the interior and the outer region are taken as

$$\nu_{1\ell} = \alpha_1 + \beta_1\ell, \quad \nu_{2\ell} = \alpha_2 + \beta_2\ell(\ell+1). \tag{12}$$

The decay rate has been calculated by

$$P = P_0 T,$$

where the assault frequency P_0 is calculated from the zero point vibration energy $E_\nu = 1/2hP_0$. The zero point vibration energy used in the present calculations are the same as those described in [19] immediately after eq. (4). The half-life t is calculated as

$$t = \log_{\rm e} 2/P. \tag{13}$$

The transmission coefficient can also be calculated in the WKB method from the expression

$$T = \exp\left[-2\int_{r_1}^{r_2} k(r){\rm d}r\right] \tag{14}$$

with

$$k(r) = \sqrt{\frac{2\mu}{\hbar^2}[V(r) - Q]}. \tag{15}$$

Here $V(r)$ is the potential barrier. The inner and outer turning points r_1 and r_2 respectively are determined using the experimental Q value of the decay in equation $V(r) = Q$.

3. Model parameters

The above potential has six parameters λ_1, ν_1, V_{01} and λ_2, ν_2, V_{02}, describing the potential on either side of the merger. These parameters are connected to each other through the expressions obtained by equating the two side of the barrier at $r = C_t(\rho = 0)$

$$V_B = V_{01}\left[\lambda_1^2\left(\nu_1^2 + \nu_1 - \frac{1}{2}\right) + \frac{1}{2}\right] = V_{02}\left[\lambda_2^2\left(\nu_2^2 + \nu_2 - \frac{1}{2}\right) + \frac{1}{2}\right].$$

This composite barrier can become symmetric, asymmetric, more flat or less flat on either side depending on the values of the above parameters. In choosing the model parameters we are guided by the following considerations. In naive calculation the barrier height should correspond to the Coulomb plus the centrifugal potentials. For $A = 105$–171, the combined Coulomb and centrifugal potentials give rise to barriers of the order of 15 MeV [2]. But the earlier studies [13,14] show that inclusion of nuclear potential and various renormalization processes tend to reduce the barrier height substantially. For ^{105}Sb, Becchetti and Greenlees [20] and Balasubramanium and Arunachalam [21] have estimated the barrier height at the touching radius to be nearly 10 MeV for $\ell = 2$ state, and 7 MeV for $\ell = 0$ state. Barrier height for $\ell = 2$ state in ^{156}Ta has also been estimated to be ≈10 MeV [9]. In the present work

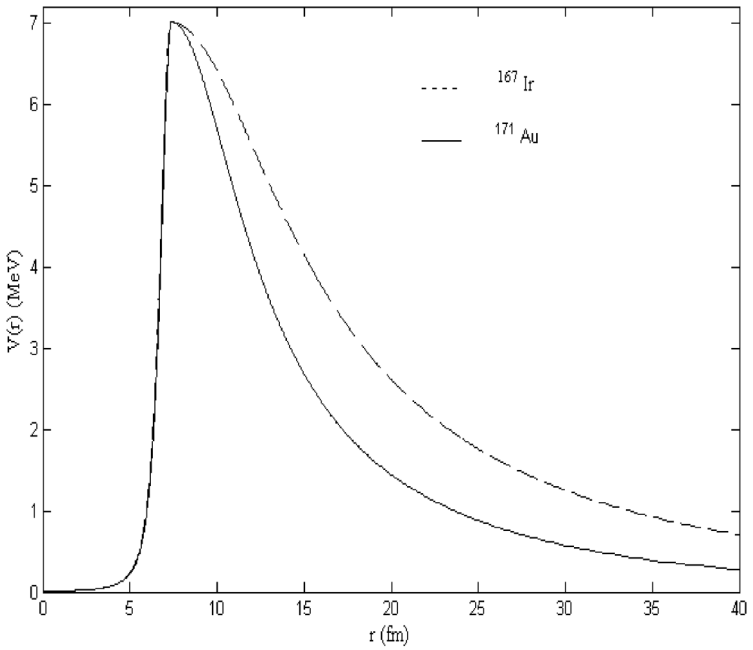

Figure 1. Potential barriers for $\ell = 0$ state proton emission as a function of r for the smallest and the largest values of $\nu_{2\ell}$ which correspond to the nuclei ^{167}Ir and ^{171}Au respectively. Potential barriers for all the remaining nuclei have similar nature.

Table 1. The logarithm of half-lives of various proton emitters.

						$\log_{10}(t)$ (s)				
							Experi-	Other work		
Nucleus	ℓ	Q (MeV)	E_ν (MeV)	P_0 ($\times 10^{19}$ s^{-1})	$\nu_{2\ell}$	Calculated	mental Ref. [21]	Ref. [17]	Ref. [9]	Ref. [2]
^{105}Sb	2	0.491	0.053	2.53	13.71	2.053	2.049	2.10	2.06	–
^{109}I	2	0.829	0.088	4.2	10.73	−4.01	−4.00	−4.30	−4.46	−5.00
^{157}Ta	0	0.947	0.101	4.86	12.54	−0.519	−0.523	−0.05	−1.22	−0.66
^{156}Ta	2	1.028	0.087	4.2	12.51	−0.609	−0.62	−0.49	−0.93	−1.01
^{167}Ir	0	1.086	0.114	5.58	12.24	−0.945	−0.959	−0.88	−1.55	−1.44
^{156}Ta*	5	1.130	0.095	4.6	13.36	0.950	0.949	–	0.79	–
^{146}Tm	5	1.140	0.096	4.65	12.5	−0.641	−0.63	−0.91	−0.69	−0.46
^{166}Ir	2	1.168	0.098	4.77	12.45	−0.827	−0.824	−1.19	−0.98	−1.68
^{161}Re	0	1.214	0.129	6.24	10.85	−3.443	−3.432	−3.16	−3.64	−3.72
^{151}Lu	5	1.255	0.133	6.45	13.44	0.84	0.89	−0.88	−1.44	−1.22
^{167}Ir*	5	1.261	0.134	6.5	13.45	0.879	0.875	–	−2.69	0.30
^{150}Lu	5	1.283	0.108	5.24	12.28	−1.189	−1.180	−1.17	−1.74	−1.51
^{150}Lu*	2	1.317	0.112	5.4	10.31	−4.545	−4.523	–	–	–
^{161}Re*	5	1.338	0.142	6.9	12.74	−0.495	−0.488	–	−1.07	−1.00
^{166}Ir*	5	1.340	0.113	5.5	12.91	−0.085	−0.076	–	−0.55	−0.48
^{171}Au	0	1.469	0.157	7.6	10.0	−4.75	−4.77	–	–	–
^{171}Au	5	1.718	0.183	8.8	11.65	−2.67	−2.654	−3.21	−3.22	−3.41
^{165}Ir	5	1.733	0.184	8.91	11.1	−3.48	−3.469	−3.73	−4.17	−3.96

*Denotes isomeric state of the parent nucleus.

we have taken $V_{\rm B} = 7$ MeV for $\ell = 0$ for all the nuclei considered and height for higher ℓ states has been estimated by adding centrifugal term $[\hbar^2/2\mu]\ell(\ell+1)/C_{\rm t}^2$ to $V_{\rm B}$. As λ increases potential falls off more sharply, whereas the range of the potential increases with ν. Earlier studies have shown that the inner barrier is very narrow and sharply falling [9]. Shanmugam *et al* [10,15] and Duarte *et al* [22] have also shown in independent studies that the width of the inner barrier decreases with the decrease in the mass of the emitted particle. In view of this we have fixed $\lambda_1 = 0.6, \nu_{1\ell} = 0.5$ indicative of a narrow sharply falling potential. The contribution of the inner barrier to the half-life values being small, $\nu_{1\ell}$ is kept constant for all ℓ values. As the outer potential barrier simulates the slowly falling long-ranged Coulomb barrier for $\ell = 0$, we have fixed $\lambda_2 = 0.4$ and have varied $\nu_{2\ell}$ starting from a large base value of 10 to 14 to reproduce the experimental data. The same procedure has been adopted for higher ℓ states as well with barrier height $V_{\rm B}$ replaced by $V_{{\rm B}\ell}$.

4. Results

The half-lives of proton emitters in the range $105 \le A \le 171$ are shown in table 1 and compared with the experimental data and other calculations. In all the cases good agreement with experimental results is obtained by varying the parameter $\nu_{2\ell}$ which controls the range of the potential for fixed barrier height. The resulting barriers for the limiting values of $\nu_{2\ell}$ are shown in figure 1 for $\ell = 0$. Variation of half-lives of proton emitters with Q values is shown in figure 2. It should be mentioned that the choice of the parameters is not unique. A change in the value

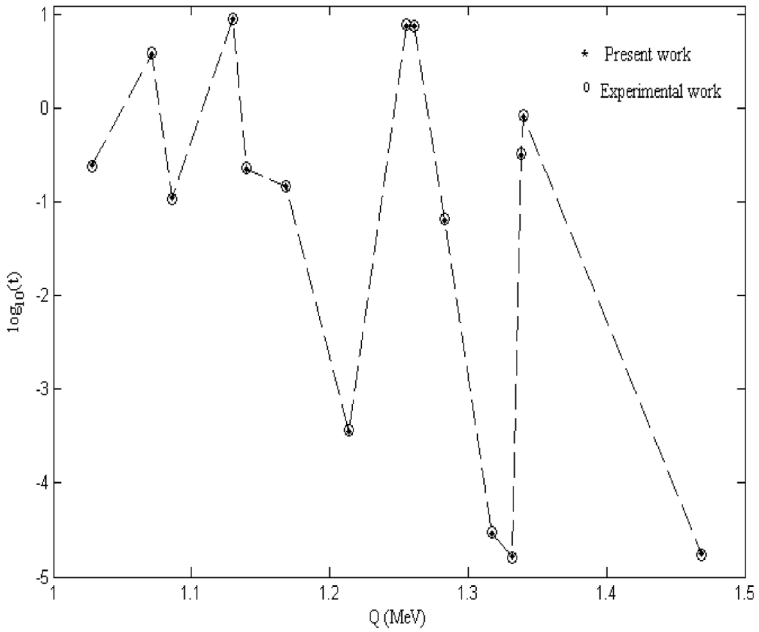

Figure 2. The logarithm of half-lives of various proton emitters as a function of Q.

of λ can reproduce the experimental results equally well, provided the ratio λ/ν is held constant with the constraint that $\lambda/\nu < 1.4$. For larger ratios the single barrier starts to become a double barrier with the pocket at the middle [11]. It is observed that the $\nu_{2\ell}$ values obtained from best fit to experimental data vary almost inversely with $\sqrt{Q}$ for the same ℓ but different nuclei. Taking $\nu_{2\ell}$ for smallest Q values as reference, $\nu'_{2\ell}$s are calculated from the relation $\nu'_{2\ell} = [\sqrt{(Q/Q')}]\nu_{2\ell}$ for constant ℓ. These values are compared with the $\nu_{2\ell}$ values obtained from best fit to the experimental half-life values in table 2. From eq. (12) constant $\alpha_2 = \nu_{2\ell}$ for $\ell = 0$ and β_2s are obtained by putting the values of $\nu_{2\ell}$ for different ℓs. These values are shown in table 3 for different nuclei. The constant β_2 ranges from 0.02 to 0.13.

5. Summary and conclusions

In conclusion we can say that whatever be the origin (microscopic or collective), in a simple picture study of proton radioactivity reduces to transmission of a particle through a potential barrier similar to the process of a very asymmetric fission. As a combined effect of all the possible modifications due to various renormalization processes one expects a dramatic change in the shape, range and asymmetry of the barrier. Earlier studies indicate that the modified barrier has a narrow tail in the inner region, parabolic shape at the top and a long Coulombic tail for all the partial waves in the outer region. The present calculation has distinct advantages

Table 2. Comparison of $\nu_{2\ell}$ values obtained from best fit to experimental data with those obtained from relation $\nu'_{2\ell} = [\sqrt{(Q/Q')}]\nu_{2\ell}$ for constant ℓ.

Nucleus	ℓ	Q (MeV)	$\nu_{2\ell}$	$\nu'_{2\ell}$
^{167}Ir	0	1.086	12.24	–
^{177}Tl	0	1.180	12.06	11.74
^{161}Re	0	1.214	10.85	11.58
^{171}Au	0	1.469	10.0	10.52
^{156}Ta	2	1.028	12.51	–
^{147}Tm	2	1.139	11.1	11.88
^{166}Ir	2	1.168	12.54	11.74
^{150}Lu	2	1.317	10.4	11.05
^{151}Lu	2	1.332	10.31	10.99
^{147}Tm	5	1.071	13.17	–
^{156}Ta	5	1.130	13.36	12.82
^{151}Lu	5	1.255	13.44	12.17
^{167}Ir	5	1.261	13.45	12.14
^{150}Lu	5	1.283	12.28	12.03
^{166}Ir	5	1.340	12.91	11.77
^{161}Re	5	1.338	12.74	11.78
^{171}Au	5	1.718	11.65	10.4

Table 3. β_2 values for different nuclei calculated from eq. (12). α_2 is equal to $\nu_{2\ell}$ for $\ell = 0$ state.

Nucleus	α_2	β_2
^{161}Re	10.85	0.06
^{167}Ir	12.24	0.04
^{171}Au	10.0	0.06
^{147}Tm	10.58	0.09
^{150}Lu	9.93	0.08
^{151}Lu	9.53	0.13
^{156}Ta	12.30	0.04
^{166}Ir	12.34	0.02

over the previous works [9,16] employing similar techniques. Firstly, in the present method it has been possible to parameterize the complete geometrical shape of the barrier. Secondly, exact expression for the transmission coefficient through the barrier has been used to calculate the half-lives whereas in the earlier studies transmission probabilities through the barrier have been calculated using WKB approximation method. In order to compare the exact transmission probabilities with those obtained in WKB method we have made calculations of transmission probabilities for different symmetric potentials. The results are shown in table 4. It is observed that the WKB method overestimates the transmission probabilities as compared to the exact value and the discrepancy increases with increasing range of the barrier. The energy of the proton $E_{\rm p} \approx [A - 1/A]Q$, where A is the mass

Table 4. Comparison of half-life values of ^{109}I obtained with the exact-transmission coefficient and with the WKB method for different symmetric potentials ($\nu_1 = \nu_2 = \nu; \lambda_1 = \lambda_2 = 0.6$) and $V_B = 10$ MeV.

	$\log_{10}(t)$ (s)	
ν	Exact	WKB
2.0	−16.122	−16.280
3.0	−14.402	−14.696
4.0	−12.729	−13.14
5.0	−11.078	−11.616
6.0	−9.439	−10.122
7.0	−7.806	−8.543
8.0	−6.178	−7.095

number of the decaying nucleus. For Q ranging between 0.5 MeV and 1.75 MeV the de Broglie wavelength of the proton lies between 20 fm $< \lambda_B <$ 42 fm and is comparable to the width of the barrier. This makes the tunneling more quantal in nature and thus the semiclassical WKB method has limited validity. Also our method of calculating the assault frequency from the zero point vibration energy data of ref. [19] is more appropriate compared to the methods used in refs [9] and [16]. Guzman *et al* [9] have used a constant value of 5×10^{20} s^{-1} for the assault frequency whereas Shanmugam *et al* [16] have estimated the assault frequency from the relative motion of the fragments in the range described by the sum of Sussmann central radii of the parent and the daughter nuclei. To sum up, the potential used in the present work is highly versatile in nature. Hitherto, a potential which parameterizes the full geometry of the proton emission barrier and also admits exact expression for the transmission coefficient has been illusive. It can also be used in parameterization of the charged particle barrier formed in the event of α-decay and also in the study of the barrier top resonances [23] in heavy ion nuclear reactions.

References

[1] S Hofmann, *Particle emission from nuclei* edited by M Ivascu and D N Poenaru (CRC, Boca Raton, FL 2, 1989) vol. 2, chap. 2

[2] S Aberg, P B Semmes and W Nazarewicz, *Phys. Rev.* **C56**, 1762 (1997)

[3] B Buck and A C Merchant, *Phys. Rev.* **C45**, 1688 (1992)

[4] A I Baz, Ya B Zel'dovich and A M Perelomov, *Scattering reactions and decay in non-relativistic quantum mechanics* (Israel Program for Scientific translations, Jerusalem, 1969)

[5] S A Gurvitz and G Kalbermann, *Phys. Rev. Lett.* **59**, 262 (1987)

[6] M Goncalves and S B Duarte, *Phys. Rev.* **C48**, 2409 (1993)

[7] O Rodriguez, F Guzmann, S B Duarte, O A P Tavares, F Garcia and M Goncalves, *Phys. Rev.* **C59**, 253 (1999)

[8] V M Strutinsky, *Nucl. Phys.* **A95**, 420 (1967)

[9] F Guzmann, M Goncalves, O A P Tavares, S B Duarte, F Garcia and O Rodriguez, *Phys. Rev.* **C59**, R 2339 (1999)
[10] G Shanmugam and B Kamalaharan, *Phys. Rev.* **C38**, 1377 (1988)
[11] B Sahu, S K Agarwalla and C S Shastry, *J. Phys A: Math. Gen.* **35**, 4349 (2002)
[12] B Sahu, G S Mallik and S K Agarwalla, *Nucl. Phys.* **A727**, 299 (2003)
[13] Y J Shi and W J Swiatecki, *Nucl. Phys.* **A438**, 45 (1985)
[14] A S Jenson and C Y Wong, *Phys. Rev* **C1**, 1321 (1970)
[15] G Shanmugam and B Kamalaharan, *Phys. Rev.* **C41**, 1742 (1990)
[16] Shanmugam *et al*, in *Proc. DAE-BRNS Symp. on Nuclear Physics, India* **B43**, 300 (2000)
[17] J R Nix, *Ann. Phys.* **41**, 52 (1967)
[18] J N Ginocchio, *Ann. Phys.* **152**, 203 (1984)
[19] D N Poenaru, W Greiner, M Ivascu, D Mazilu and I H Plonski, *Z. Phys.* **A325**, 435 (1986)
[20] F D Becchetti Jr and G W Greenlees, *Phys. Rev.* **182**, 1190 (1969)
[21] M Balasubramanium and N Arunachalam, *Phys. Rev.* **C71**, 014603 (2005)
[22] S B Duarte, O A P Tavares and M Goncalves, *Phys. Rev.* **C56**, 3414 (1997)
[23] Zafar Ahmed, *Phys. Rev.* **A47**, 4761 (1993)